Cell Reports Medicine, Volume *5*

Supplemental information

A multiomics analysis-assisted deep learning model identifies a macrophage-oriented module as a potential therapeutic target in colorectal cancer

Xuanwen Bao, Qiong Li, Dong Chen, Xiaomeng Dai, Chuan Liu, Weihong Tian, Hangyu Zhang, Yuzhi Jin, Yin Wang, Jinlin Cheng, Chunyu Lai, Chanqi Ye, Shan Xin, Xin Li, Ge Su, Yongfeng Ding, Yangyang Xiong, Jindong Xie, Vincent Tano, Yanfang Wang, Wenguang Fu, Shuiguang Deng, Weijia Fang, Jianpeng Sheng, Jian Ruan, and Peng Zhao

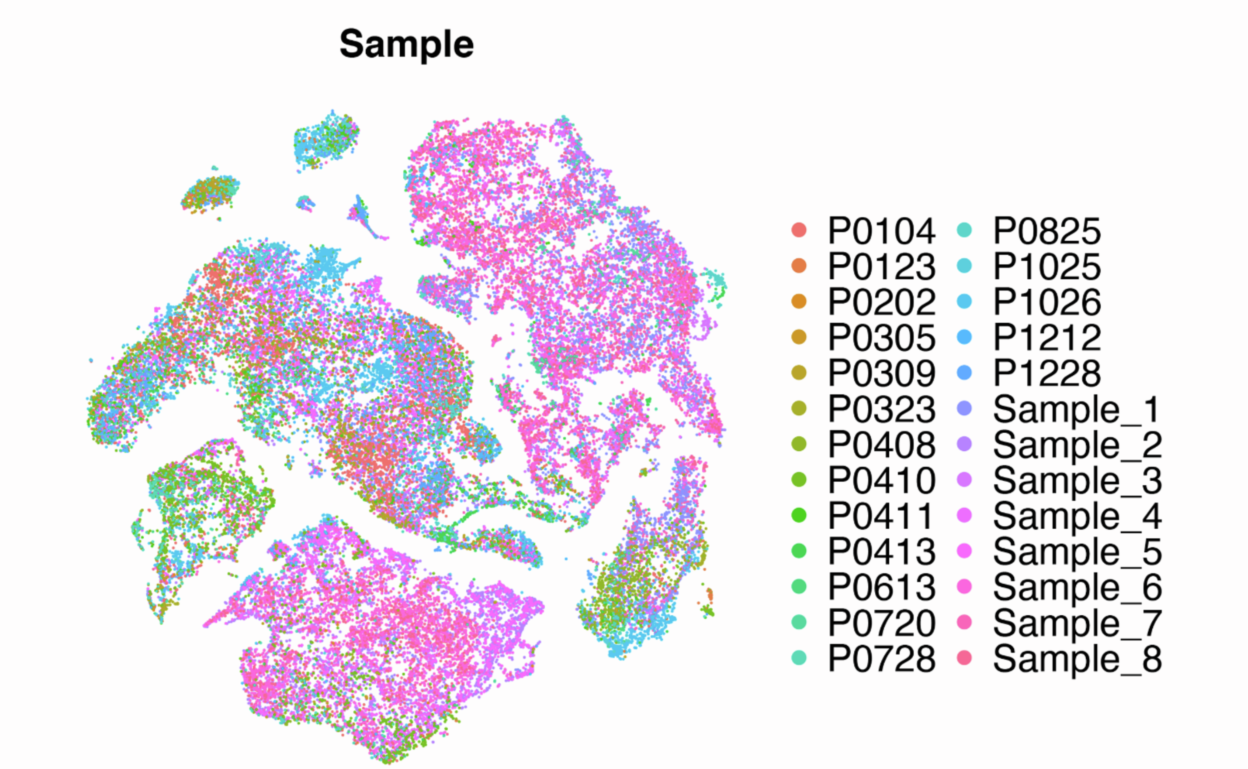

Fig. S1: The t-SNE plot coloured by CRC patients, related to Figure 1. A total of 24 patients were included for analysis. *t-SNE: t-distributed stochastic neighbour embedding; CRC: colorectal cancer.*

Figure S2

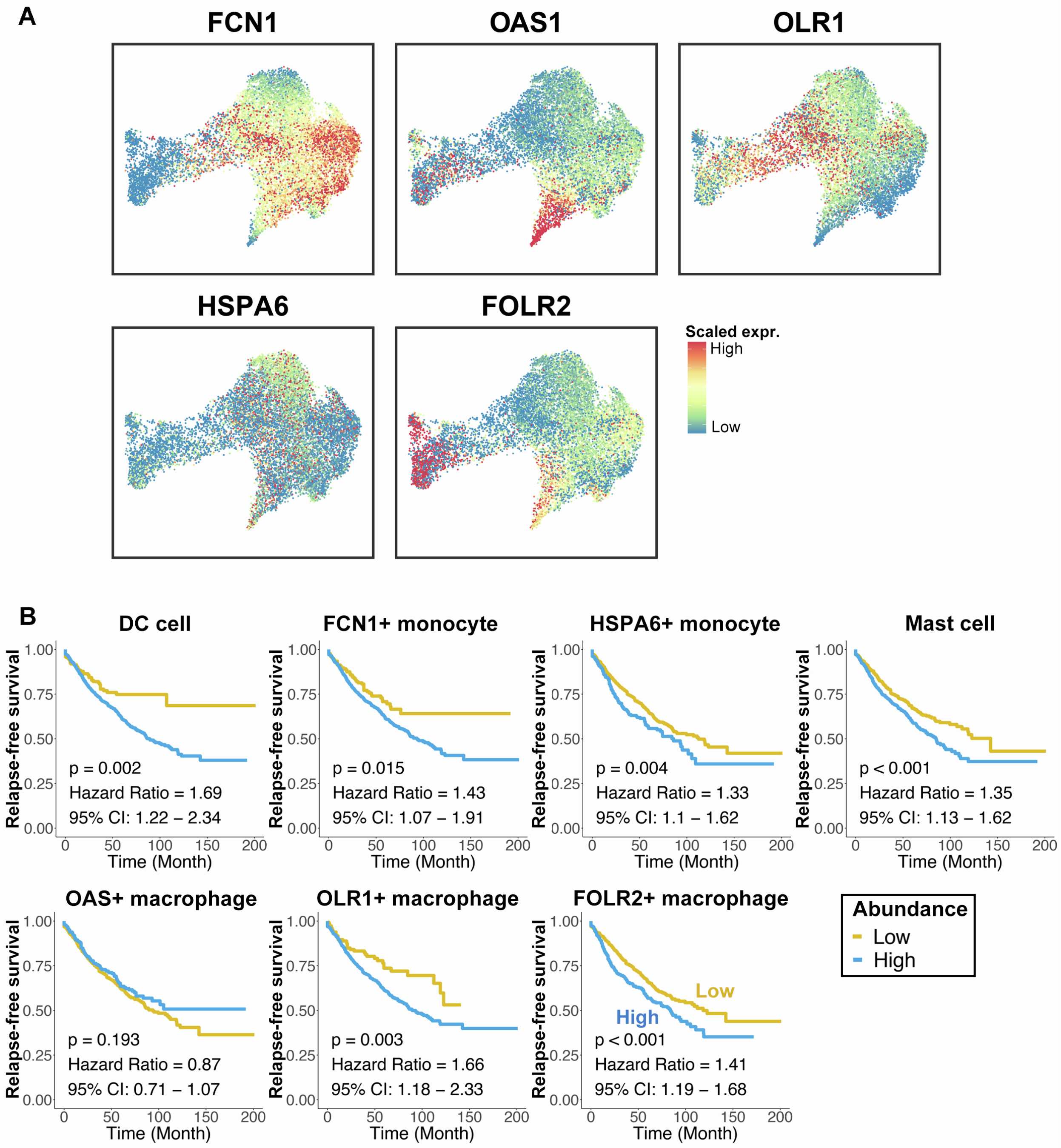

Fig. S2: The monocyte/macrophage subpopulations and their prognostic values, related to Figure 2. A.) The UMAP plot showing the expression level of the selected features in monocyte/macrophage subpopulations. B.) The association of DFS with the enrichment of each myeloid cell type. Gene signatures of myeloid cells were defined as the feature genes of each cell type and obtained from the scRNA-seq data (Pts n=1405). The cell abundance was calculated according to the gene signature for each cell type based on bulk transcriptome data using the GSVA method. *UMAP: Uniform Manifold Approximation and Projection; DFS: disease-free survival; scRNA-Seq: single-cell RNA sequencing; GSVA: gene set variation analysis, Pts: patients.*

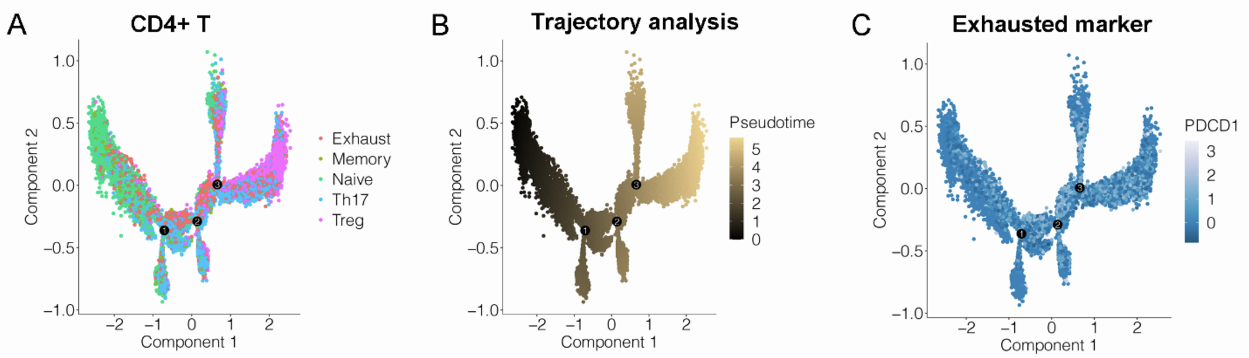

Fig. S3: The CD4+ T-cell subpopulations in CRC, related to Figure 4. A.) Trajectory inference for 5 subclusters of CD4$^+$ T cells. B.) Trajectory inference with the pseudotime score for 5 subclusters of CD4$^+$ T cells. The colour key from black to gold indicates the pseudotime score from low to high. C.) Trajectory inference with PD-1 expression for 5 subclusters of CD4$^+$ T cells. The colour key from blue to white indicates PD-1 expression from low to high. *CRC: colorectal cancer.*

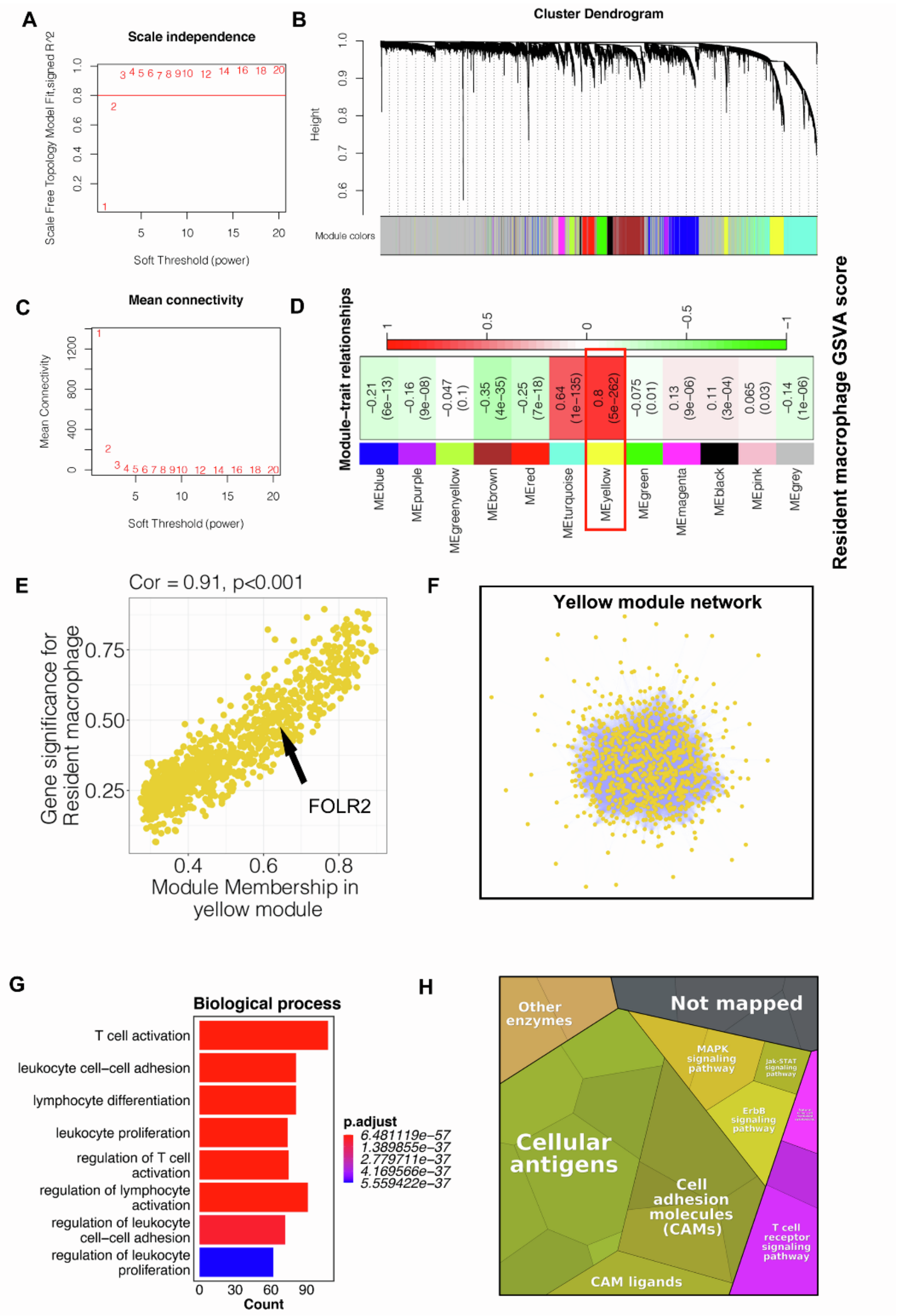

Fig. S4: Optimal soft threshold selection and sample clustering in WGCNA, related to Figure 5. A.) A power of $\beta = 3$ was chosen as the optimal soft threshold to ensure scale-free coexpression. B.) A power of $\beta = 3$ represents low mean connectivity in the WGCNA model. C.) The clustering of gene modules in WGCNA. D.) The association between identified modules and FOLR2$^+$ macrophage abundance calculated with the FOLR2$^+$ macrophage gene signature on the bulk transcriptome. The colour key from green to red indicates the relative correlation level from low to high. E.) The correlation between gene significance for FOLR2$^+$ macrophages and module membership in the yellow module. The black arrow indicates that FOLR2 is involved in the yellow module. Network clustering identified 11 non-grey (meaningful) gene modules. F.) The gene network in the yellow module. G.) Gene ontology analysis based on the genes within the yellow module (FOLR2$^+$ macrophage-related module) indicating the enriched biological process. H.) Proteomaps pathway analysis of genes within the yellow module (FOLR2$^+$ macrophage-related module). Each small polygon corresponds to a single KEGG pathway, and the size correlates with the number of genes involved in the pathway. *WGCNA: weighted gene coexpression network analysis, KEGG: Kyoto Encyclopedia of Genes and Genomes.*

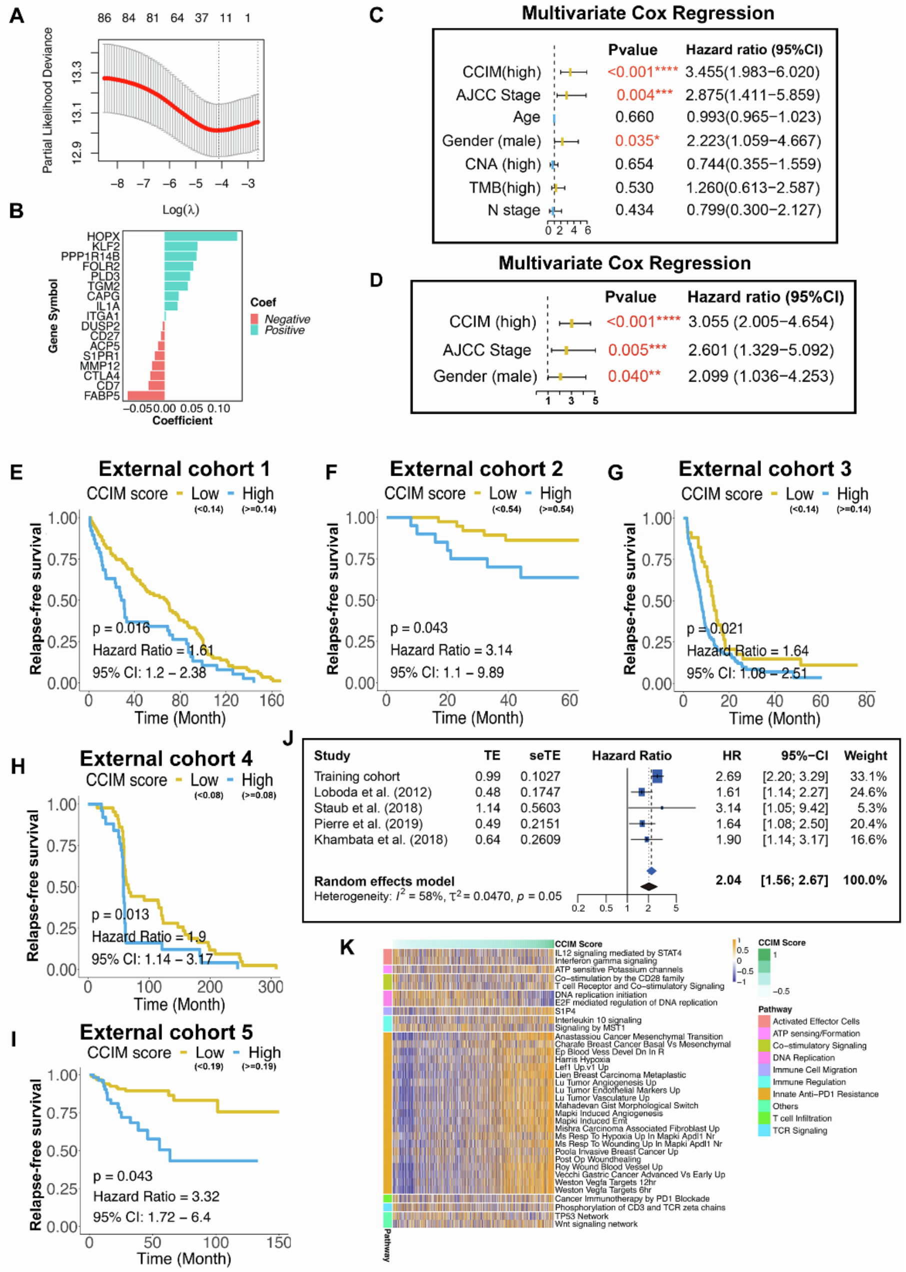

Multivariate Cox Regression

	Pvalue	Hazard ratio (95%CI)
CCIM(high)	<0.001****	3.455(1.983−6.020)
AJCC Stage	0.004***	2.875(1.411−5.859)
Age	0.660	0.993(0.965−1.023)
Gender (male)	0.035*	2.223(1.059−4.667)
CNA (high)	0.654	0.744(0.355−1.559)
TMB(high)	0.530	1.260(0.613−2.587)
N stage	0.434	0.799(0.300−2.127)

Multivariate Cox Regression

	Pvalue	Hazard ratio (95%CI)
CCIM (high)	<0.001****	3.055 (2.005−4.654)
AJCC Stage	0.005***	2.601 (1.329−5.092)
Gender (male)	0.040**	2.099 (1.036−4.253)

Study	TE	seTE	HR	95%−CI	Weight
Training cohort	0.99	0.1027	2.69	[2.20; 3.29]	33.1%
Loboda et al. (2012)	0.48	0.1747	1.61	[1.14; 2.27]	24.6%
Staub et al. (2018)	1.14	0.5603	3.14	[1.05; 9.42]	5.3%
Pierre et al. (2019)	0.49	0.2151	1.64	[1.08; 2.50]	20.4%
Khambata et al. (2018)	0.64	0.2609	1.90	[1.14; 3.17]	16.6%
Random effects model			**2.04**	**[1.56; 2.67]**	**100.0%**

Heterogeneity: $I^2 = 58\%$, $\tau^2 = 0.0470$, $p = 0.05$

Fig. S5: Construction of the CCIM scoring system, related to Figure 5. A.) The LASSO Cox regression model was used to identify the most robust markers. B.) Distribution of LASSO coefficients of the gene signature. C.) Multivariate survival analysis of the CCIM score and other clinicopathological features in the TCGA-CRC cohort. D.) Multivariate survival analysis of the CCIM score and other significant clinicopathological features in the TCGA-CRC cohort. E.) The CCIM score stratified patients with poor prognosis in independent CRC cohort #1 (GSE28722) (Pts n = 125). F.) The CCIM score stratified patients with poor prognosis in independent CRC cohort #2 (GSE12945) (Pts n = 62). G.) The CCIM score stratified patients with a poor prognosis in independent CRC cohort #3 (GSE72970) (Pts n = 124). H.) The CCIM score stratified patients with a poor prognosis in independent CRC cohort #4 (GSE5851) (Pts n = 80). For Figure S5E-S5I best-cutoff method was applied for generating the CCIM high and low group. I.) The CCIM score stratified patients with a poor prognosis in independent CRC cohort #5 (TCGA-CRC) (Pts n = 274). J.) Meta-analysis for the training and testing cohorts. Immune-related pathway alterations in patients with distinct CCIM scores. K.) The pathway alterations were assessed with the GSVA method using their gene sets. *CCIM: colorectal cancer immunosuppressive module; LASSO: least absolute shrinkage and selection operator, CRC: colorectal cancer; pts: patients.*

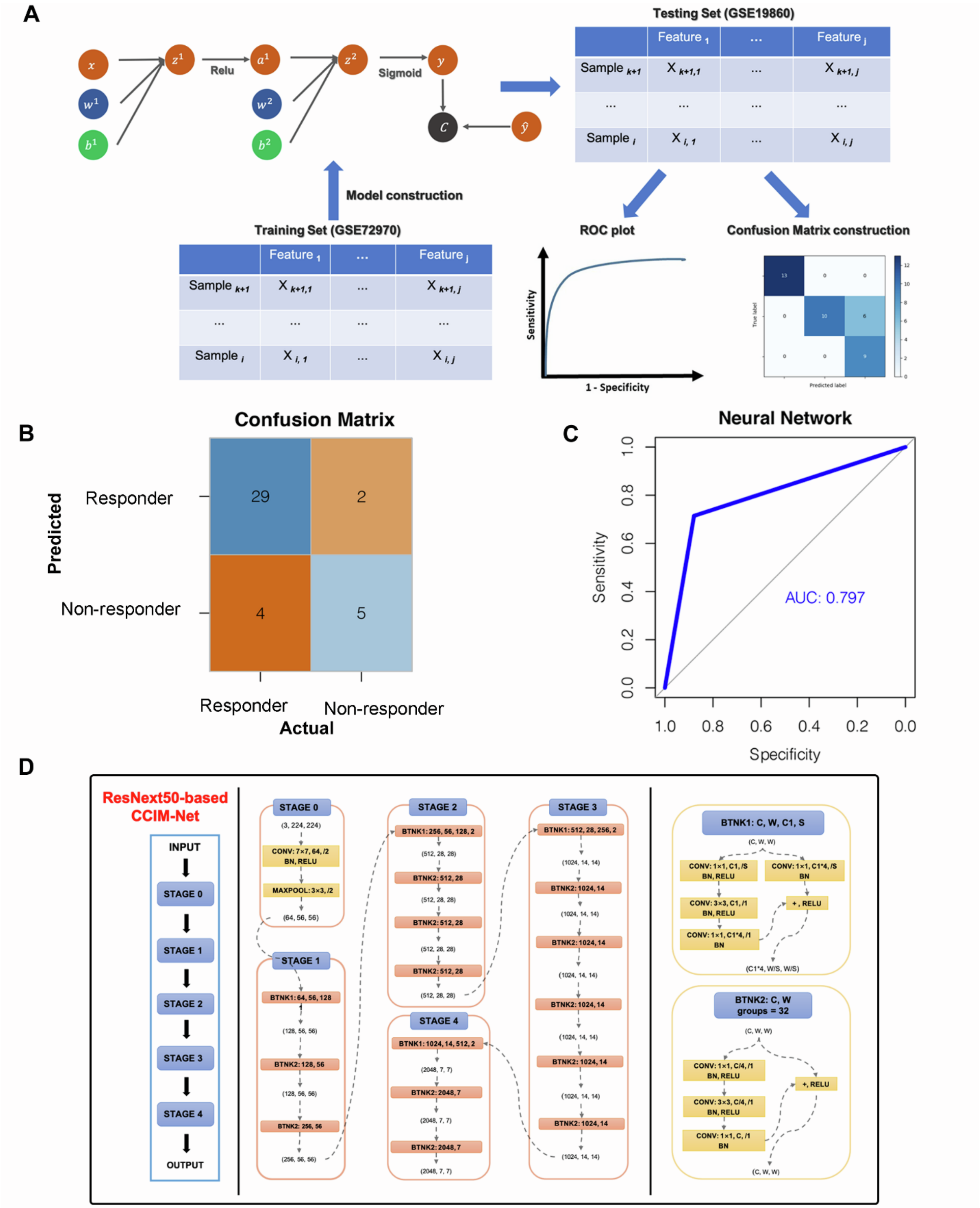

Fig. S6: A FOLR2$^+$ macrophage signature-based neural network model predicts the chemotherapy response, related to Figure 6. A.) Schematic illustration of FOLR2$^+$ macrophage signature prediction model construction and validation. B.) The confusion matrix for predicting the chemotherapy response by the FOLR2-RM model in an external cohort. The column indicates the predicted response, while the row represents the actual response. C.) The ROC analysis indicates the high sensitivity and specificity of the FOLR2-RM model. D.) The construction process of CCIM-Net by Resnext50. *ROC: receiver operating characteristic; FOLR2-RM model: FOLR2$^+$ macrophage-based model.*

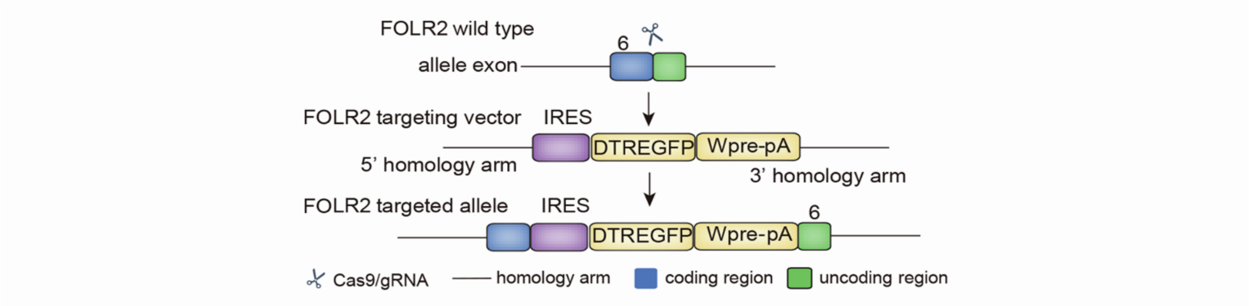

Fig. S7: The genomic schematic of editing the FOLR2-DTR-eGFP mice and gating strategy, related to Figure 7. The IRES-DTR-EGFP fusion gene was inserted into the 3'-UTR region of the FOLR2 gene locus.

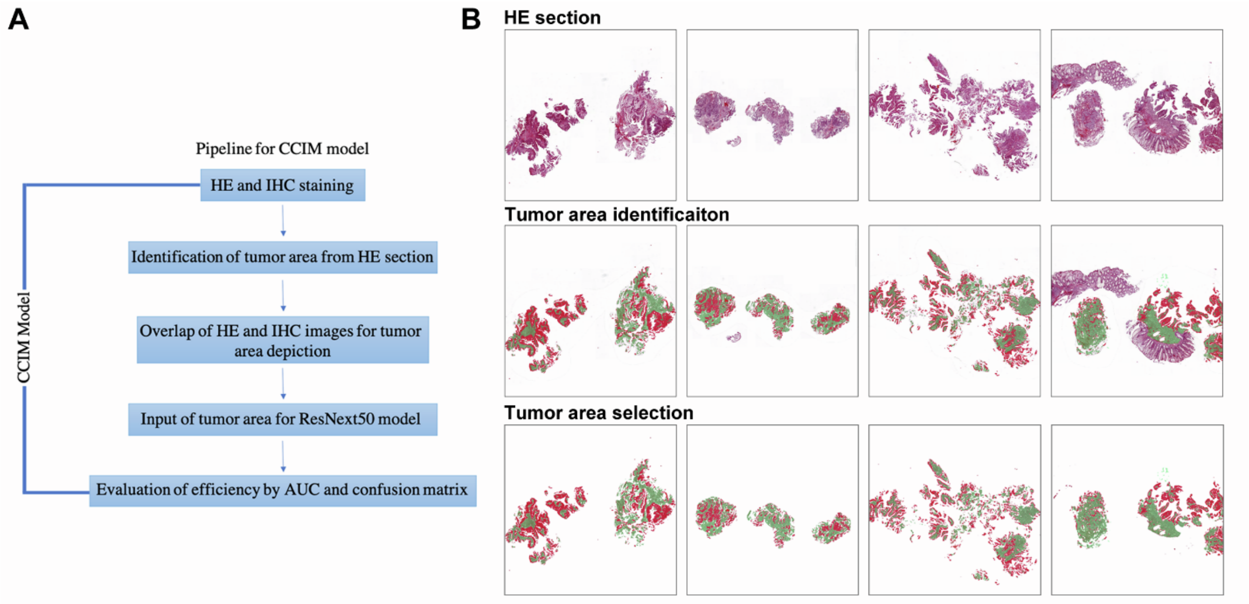

Fig. S8: The pipeline for the CCIM analysis, related to Figure 6. A.) The workflow for the deep learning pipeline in our manuscript. B.) The HE staining showing the identified tumor tissues (red indicates tumor cells and green indicates stroma cells) and para-tumor tissues on slides.

Table S1. Feature genes of myeloid cells. Related to Figure 2.

p_val	avg_log2FC	p_val_adj	cluster	gene
0	2.703467872	0	FOLR2$^+$ macrophage	APOE
0	2.569652735	0	FOLR2$^+$ macrophage	C1QC
0	2.540618403	0	FOLR2$^+$ macrophage	C1QB
0	2.520762997	0	FOLR2$^+$ macrophage	APOC1
0	2.478060246	0	FOLR2$^+$ macrophage	C1QA
0	2.156237286	0	FOLR2$^+$ macrophage	GPNMB
0	2.114256761	0	FOLR2$^+$ macrophage	RNASE1
0	1.806018055	0	FOLR2$^+$ macrophage	LGMN
0	1.702743808	0	FOLR2$^+$ macrophage	TREM2
0	1.63946639	0	FOLR2$^+$ macrophage	MSR1
0	1.790280153	0	OAS$^+$ macrophage	IFI44L
0	1.38366812	0	OAS$^+$ macrophage	OAS1
0	1.367907875	0	OAS$^+$ macrophage	OAS3
0	1.200912655	0	OAS$^+$ macrophage	CXCL10
1.74E-304	1.251750284	3.47E-301	OAS$^+$ macrophage	OASL
1.14E-280	1.740158953	2.28E-277	OAS$^+$ macrophage	TNFSF10
5.00E-272	2.076296858	9.99E-269	OAS$^+$ macrophage	MX1
1.48E-258	1.910414263	2.96E-255	OAS$^+$ macrophage	LY6E
1.89E-228	1.618872411	3.77E-225	OAS$^+$ macrophage	MT2A
1.87E-212	2.16275357	3.73E-209	OAS$^+$ macrophage	IFIT1
0	4.326570465	0	Mast cell	TPSAB1
0	4.151640883	0	Mast cell	TPSB2
0	3.719794919	0	Mast cell	CPA3
0	3.528531605	0	Mast cell	CLU
0	3.179552215	0	Mast cell	HPGDS
0	3.08481101	0	Mast cell	MS4A2
0	2.956581136	0	Mast cell	GATA2
0	2.915095278	0	Mast cell	LTC4S
3.13E-298	2.22089356	6.27E-295	Mast cell	CD9
5.56E-288	2.600934127	1.11E-284	Mast cell	VWA5A
0	2.314578538	0	FCN1$^+$ monocytes	S100A12
0	1.675024369	0	FCN1$^+$ monocytes	FCN1
0	1.443611669	0	FCN1$^+$ monocytes	RBP7
0	1.407530861	0	FCN1$^+$ monocytes	VCAN
0	1.224845612	0	FCN1$^+$ monocytes	CSTA
0	1.201167533	0	FCN1$^+$ monocytes	S100A8
0	1.109381689	0	FCN1$^+$ monocytes	CLEC12A
0	1.064708839	0	FCN1$^+$ monocytes	CFP
0	1.047715341	0	FCN1$^+$ monocytes	S100A9

0	1.01710355	0	FCN1$^+$ monocytes	PLBD1
0	1.806616701	0	OLR1$^+$ macrophage	CCL20
0	1.371324968	0	OLR1$^+$ macrophage	CXCL3
0	1.328000606	0	OLR1$^+$ macrophage	PLIN2
0	1.313447691	0	OLR1$^+$ macrophage	G0S2
0	1.229211049	0	OLR1$^+$ macrophage	NLRP3
0	1.212277595	0	OLR1$^+$ macrophage	CXCL8
0	1.168625057	0	OLR1$^+$ macrophage	UPP1
0	1.150691165	0	OLR1$^+$ macrophage	EREG
1.02E-292	1.432863049	2.04E-289	OLR1$^+$ macrophage	OLR1
2.09E-275	1.019056865	4.17E-272	OLR1$^+$ macrophage	TIMP1
0	1.631095239	0	DC cell	HLA-DQA1
0	1.390455704	0	DC cell	HLA-DQB1
0	1.364771189	0	DC cell	HLA-DMB
0	1.082507304	0	DC cell	HLA-DPB1
0	1.073994585	0	DC cell	HLA-DPA1
2.36E-275	1.452689755	4.72E-272	DC cell	PPA1
8.42E-202	1.153697115	1.68E-198	DC cell	GPR183
3.01E-191	1.060540832	6.01E-188	DC cell	UCP2
1.86E-188	1.774782864	3.72E-185	DC cell	CLEC10A
2.28E-170	1.211102005	4.55E-167	DC cell	CPVL
2.46E-124	0.801642856	4.93E-121	HSPA6$^+$ monocytes	PI3
5.59E-69	0.751508145	1.12E-65	HSPA6$^+$ monocytes	SLPI
1.04E-52	0.508773665	2.08E-49	HSPA6$^+$ monocytes	LRRC25
1.15E-37	0.499143034	2.30E-34	HSPA6$^+$ monocytes	FOS
7.02E-37	0.767185495	1.40E-33	HSPA6$^+$ monocytes	LRG1
8.01E-33	0.457828519	1.60E-29	HSPA6$^+$ monocytes	S100A6
4.74E-32	0.633038698	9.49E-29	HSPA6$^+$ monocytes	ZFAND2A
3.00E-27	0.479852005	6.00E-24	HSPA6$^+$ monocytes	CXCR4
2.10E-25	0.874316719	4.21E-22	HSPA6$^+$ monocytes	HSPA6
7.76E-24	0.598128716	1.55E-20	HSPA6$^+$ monocytes	HCAR3

Table S2. Feature genes of CD4$^+$ T cells. Related to Figure 4.

p_val	avg_log2FC	p_val_adj	cluster	gene
0	2.10186081	0	Treg	IL2RA
0	1.861650068	0	Treg	FOXP3
0	1.836449779	0	Treg	TNFRSF18
0	1.744619545	0	Treg	TNFRSF4
0	1.591211126	0	Treg	BATF
0	1.573961766	0	Treg	LAIR2
0	1.529423238	0	Treg	TNFRSF9
0	1.454852486	0	Treg	DUSP4
0	1.38027878	0	Treg	TIGIT
0	1.210566934	0	Treg	CTLA4
0	1.525099519	0	Naive	CCR7
7.99E-284	1.271369831	1.60E-280	Naive	MAL
1.40E-252	0.496372502	2.81E-249	Naive	PABPC1
6.67E-208	0.920624495	1.33E-204	Naive	PLAC8
3.22E-189	0.508841364	6.43E-186	Naive	LDHB
4.45E-178	0.702815017	8.90E-175	Naive	YPEL5
1.74E-168	0.912903959	3.49E-165	Naive	AREG
7.86E-151	0.624424222	1.57E-147	Naive	GPR183
2.12E-143	0.721272861	4.23E-140	Naive	SLC2A3
2.71E-139	0.620338115	5.42E-136	Naive	FOS
0	1.3892901	0	Th17	CCL5
0	1.188210898	0	Th17	ANXA1
0	0.931498989	0	Th17	GPR171
1.79E-292	0.92752317	3.58E-289	Th17	KLRB1
2.55E-285	0.72817835	5.10E-282	Th17	IL7R
1.47E-284	0.940234127	2.94E-281	Th17	FKBP11
1.66E-283	0.953685169	3.33E-280	Th17	ID2
6.20E-280	1.011205571	1.24E-276	Th17	ANKRD28
4.59E-244	0.954412521	9.18E-241	Th17	GPR65
1.32E-234	0.970994223	2.63E-231	Th17	IL17A
1.45E-149	1.288450419	2.90E-146	Exhaust	PDCD1
4.28E-146	0.937759753	8.55E-143	Exhaust	TIGIT
9.08E-146	1.444081009	1.82E-142	Exhaust	TOX2
9.98E-127	1.282741513	2.00E-123	Exhaust	ICA1
5.59E-115	0.767821251	1.12E-111	Exhaust	LIMS1
3.93E-107	0.888092037	7.86E-104	Exhaust	TBC1D4
8.71E-105	0.872393829	1.74E-101	Exhaust	SH2D1A
6.01E-100	0.763778656	1.20E-96	Exhaust	MAF
2.05E-90	0.622782937	4.09E-87	Exhaust	ITM2A

5.32E-75	1.568188242	1.06E-71	Exhaust	CXCL13
4.84E-249	2.754926942	9.68E-246	Memory	TMEM204
5.75E-20	0.639291027	1.15E-16	Memory	GIMAP7
4.56E-17	0.49324668	9.11E-14	Memory	RPS4Y1
1.80E-16	0.59686813	3.61E-13	Memory	GIMAP4
1.82E-14	0.392548485	3.63E-11	Memory	IL7R
8.93E-14	0.691505443	1.79E-10	Memory	PLAC8
7.00E-13	0.27137293	1.40E-09	Memory	LDHB
1.75E-12	0.403172704	3.50E-09	Memory	ANXA1
2.72E-08	0.410434881	5.43E-05	Memory	TRAT1
1.42E-07	0.639850827	0.000284346	Memory	CCR7

Table S3. Feature genes of CD8$^+$ T cells. Related to Figure 4.

p_val	avg_log2FC	p_val_adj	cluster	gene
0	2.200701212	0	Effector memory	GZMK
0	1.30252866	0	Effector memory	SH2D1A
0	1.21816221	0	Effector memory	ITGB2
0	1.023573045	0	Effector memory	CD27
0	0.830763101	0	Effector memory	CD74
8.73E-271	0.867991915	1.75E-267	Effector memory	HLA-DPB1
7.68E-255	1.167004015	1.54E-251	Effector memory	GZMH
8.49E-215	0.782787791	1.70E-211	Effector memory	GPR183
2.64E-200	0.678554339	5.27E-197	Effector memory	CCR7
5.64E-177	0.864636785	1.13E-173	Effector memory	HLA-DRA
0	1.894683286	0	Exhaust	TMIGD2
0	1.85965092	0	Exhaust	CD160
0	1.459115224	0	Exhaust	LDLRAD4
0	1.317366481	0	Exhaust	HOPX
0	1.169102265	0	Exhaust	KLRD1
0	0.937885175	0	Exhaust	CD7
1.54E-291	1.66042112	3.09E-288	Exhaust	SPRY1
6.94E-291	1.146572869	1.39E-287	Exhaust	GPR65
9.10E-285	1.224418415	1.82E-281	Exhaust	ITGA1
3.62E-283	0.908541583	7.24E-280	Exhaust	CD63
3.02E-196	1.276163725	6.03E-193	Exhaust NKT	HAVCR2
2.89E-175	1.846789084	5.78E-172	Exhaust NKT	CXCL13
3.98E-171	1.839221638	7.96E-168	Exhaust NKT	GNLY
4.34E-170	1.093208479	8.67E-167	Exhaust NKT	ENTPD1
5.70E-156	1.101150394	1.14E-152	Exhaust NKT	PHLDA1
4.11E-154	1.284014249	8.23E-151	Exhaust NKT	GZMB
5.07E-136	0.995602299	1.01E-132	Exhaust NKT	DUSP4
5.73E-125	0.821779459	1.15E-121	Exhaust NKT	CD70
2.60E-119	0.766485572	5.19E-116	Exhaust NKT	ACP5
2.37E-89	0.776973157	4.74E-86	Exhaust NKT	CD9
0	2.405764276	0	Tissue resident	ZNF683
7.47E-49	0.509462029	1.49E-45	Tissue resident	S100A4
8.58E-39	0.54810102	1.72E-35	Tissue resident	GZMB
6.50E-33	0.583926417	1.30E-29	Tissue resident	GZMH
1.34E-31	0.530854143	2.68E-28	Tissue resident	LGALS1
2.51E-27	0.368744099	5.02E-24	Tissue resident	CAPG
3.64E-25	0.487994878	7.27E-22	Tissue resident	HLA-DRA
5.12E-25	0.346868476	1.02E-21	Tissue resident	S100A6
5.16E-24	0.416649564	1.03E-20	Tissue resident	CLU

1.57E-23	0.375491203	3.15E-20	Tissue resident	MT2A
2.62E-165	2.310225713	5.24E-162	Tolerant	DKK3
3.50E-65	1.196683211	7.00E-62	Tolerant	GZMK
3.77E-30	0.758749457	7.53E-27	Tolerant	SH2D1A
2.53E-26	0.759367969	5.07E-23	Tolerant	CD27
9.11E-24	0.510185222	1.82E-20	Tolerant	CST7
3.34E-22	0.571940512	6.69E-19	Tolerant	GPR183
6.39E-19	0.58504908	1.28E-15	Tolerant	ITGB2
5.54E-18	0.529356191	1.11E-14	Tolerant	TRAT1
5.87E-17	0.414195428	1.17E-13	Tolerant	DUSP2
1.14E-15	0.66396579	2.27E-12	Tolerant	CCR7

Table S4. Cell-cell interaction pairs. Related to Figure 5.

Ligand	Receptor	Interaction.type	LRscore	Ligand_cell	Receptor_cell
CD86	CTLA4	paracrine	0.958	FOLR2$^+$ macrophage	Treg
CXCL16	CXCR6	paracrine	0.946	FOLR2$^+$ macrophage	Treg
MRC1	PTPRC	paracrine	0.933	FOLR2$^+$ macrophage	Treg
CD80	CTLA4	paracrine	0.933	FOLR2$^+$ macrophage	Treg
SPP1	ITGA4	paracrine	0.915	FOLR2$^+$ macrophage	Treg
CD14	ITGA4	paracrine	0.913	FOLR2$^+$ macrophage	Treg
ICAM1	IL2RG	paracrine	0.900	FOLR2$^+$ macrophage	Treg
LGALS1	PTPRC	paracrine	0.899	FOLR2$^+$ macrophage	Treg
IL18	IL18R1	paracrine	0.894	FOLR2$^+$ macrophage	Treg
CCL20	CCR6	paracrine	0.893	FOLR2$^+$ macrophage	Treg
F13A1	ITGA4	paracrine	0.891	FOLR2$^+$ macrophage	Treg
FN1	ITGA4	paracrine	0.890	FOLR2$^+$ macrophage	Treg
IL1RN	IL1R1	paracrine	0.881	FOLR2$^+$ macrophage	Treg
IL1B	IL1R1	paracrine	0.879	FOLR2$^+$ macrophage	Treg
VCAN	SELL	paracrine	0.851	FOLR2$^+$ macrophage	Treg
TGM2	ITGA4	paracrine	0.841	FOLR2$^+$ macrophage	Treg
CALM2	SELL	paracrine	0.832	FOLR2$^+$ macrophage	Treg
VCAN	ITGA4	paracrine	0.819	FOLR2$^+$ macrophage	Treg
THBS1	ITGA4	paracrine	0.789	FOLR2$^+$ macrophage	Treg
SPP1	S1PR1	paracrine	0.750	FOLR2$^+$ macrophage	Treg
C3	IFITM1	paracrine	0.737	FOLR2$^+$ macrophage	Treg
IL1A	IL1R1	paracrine	0.697	FOLR2$^+$ macrophage	Treg
MRC1	PTPRC	paracrine	0.935	FOLR2$^+$ macrophage	Exhaust CD8$^+$ T
CXCL16	CXCR6	paracrine	0.922	FOLR2$^+$ macrophage	Exhaust CD8$^+$ T
LGALS1	CD69	paracrine	0.919	FOLR2$^+$ macrophage	Exhaust CD8$^+$ T
LGALS1	PTPRC	paracrine	0.902	FOLR2$^+$ macrophage	Exhaust CD8$^+$ T
SPP1	ITGA4	paracrine	0.902	FOLR2$^+$ macrophage	Exhaust CD8$^+$ T
CD14	ITGA4	paracrine	0.899	FOLR2$^+$ macrophage	Exhaust CD8$^+$ T
ICAM1	IL2RG	paracrine	0.883	FOLR2$^+$ macrophage	Exhaust CD8$^+$ T
IL18	CD48	paracrine	0.876	FOLR2$^+$ macrophage	Exhaust CD8$^+$ T
F13A1	ITGA4	paracrine	0.874	FOLR2$^+$ macrophage	Exhaust CD8$^+$ T
FN1	ITGA4	paracrine	0.872	FOLR2$^+$ macrophage	Exhaust CD8$^+$ T
IL18	IL18R1	paracrine	0.818	FOLR2$^+$ macrophage	Exhaust CD8$^+$ T
TGM2	ITGA4	paracrine	0.818	FOLR2$^+$ macrophage	Exhaust CD8$^+$ T
VCAN	ITGA4	paracrine	0.794	FOLR2$^+$ macrophage	Exhaust CD8$^+$ T
THBS1	ITGA4	paracrine	0.760	FOLR2$^+$ macrophage	Exhaust CD8$^+$ T
C3	IFITM1	paracrine	0.724	FOLR2$^+$ macrophage	Exhaust CD8$^+$ T
CD86	CTLA4	paracrine	0.940	FOLR2$^+$ macrophage	Exhaust CD4$^+$ T
MRC1	PTPRC	paracrine	0.937	FOLR2$^+$ macrophage	Exhaust CD4$^+$ T

SPP1	ITGA4	paracrine	0.920	FOLR2$^+$ macrophage	Exhaust CD4$^+$ T
CD14	ITGA4	paracrine	0.918	FOLR2$^+$ macrophage	Exhaust CD4$^+$ T
CD80	CTLA4	paracrine	0.906	FOLR2$^+$ macrophage	Exhaust CD4$^+$ T
LGALS1	PTPRC	paracrine	0.905	FOLR2$^+$ macrophage	Exhaust CD4$^+$ T
CXCL16	CXCR6	paracrine	0.902	FOLR2$^+$ macrophage	Exhaust CD4$^+$ T
F13A1	ITGA4	paracrine	0.897	FOLR2$^+$ macrophage	Exhaust CD4$^+$ T
FN1	ITGA4	paracrine	0.896	FOLR2$^+$ macrophage	Exhaust CD4$^+$ T
LGALS1	CD69	paracrine	0.886	FOLR2$^+$ macrophage	Exhaust CD4$^+$ T
ICAM1	IL2RG	paracrine	0.885	FOLR2$^+$ macrophage	Exhaust CD4$^+$ T
TGM2	ITGA4	paracrine	0.850	FOLR2$^+$ macrophage	Exhaust CD4$^+$ T
VCAN	ITGA4	paracrine	0.829	FOLR2$^+$ macrophage	Exhaust CD4$^+$ T
C3	IFITM1	paracrine	0.826	FOLR2$^+$ macrophage	Exhaust CD4$^+$ T
CCL20	CCR6	paracrine	0.824	FOLR2$^+$ macrophage	Exhaust CD4$^+$ T
IL18	CD48	paracrine	0.823	FOLR2$^+$ macrophage	Exhaust CD4$^+$ T
THBS1	ITGA4	paracrine	0.799	FOLR2$^+$ macrophage	Exhaust CD4$^+$ T
SPP1	S1PR1	paracrine	0.774	FOLR2$^+$ macrophage	Exhaust CD4$^+$ T
VCAN	SELL	paracrine	0.586	FOLR2$^+$ macrophage	Exhaust CD4$^+$ T
CALM2	SELL	paracrine	0.550	FOLR2$^+$ macrophage	Exhaust CD4$^+$ T
MRC1	PTPRC	paracrine	0.940	FOLR2$^+$ macrophage	Tolerant CD8$^+$ T
LGALS1	PTPRC	paracrine	0.910	FOLR2$^+$ macrophage	Tolerant CD8$^+$ T
CXCL16	CXCR6	paracrine	0.908	FOLR2$^+$ macrophage	Tolerant CD8$^+$ T
SPP1	ITGA4	paracrine	0.902	FOLR2$^+$ macrophage	Tolerant CD8$^+$ T
CD14	ITGA4	paracrine	0.899	FOLR2$^+$ macrophage	Tolerant CD8$^+$ T
LGALS1	CD69	paracrine	0.897	FOLR2$^+$ macrophage	Tolerant CD8$^+$ T
IL18	CD48	paracrine	0.897	FOLR2$^+$ macrophage	Tolerant CD8$^+$ T
SPP1	S1PR1	paracrine	0.896	FOLR2$^+$ macrophage	Tolerant CD8$^+$ T
F13A1	ITGA4	paracrine	0.874	FOLR2$^+$ macrophage	Tolerant CD8$^+$ T
FN1	ITGA4	paracrine	0.872	FOLR2$^+$ macrophage	Tolerant CD8$^+$ T
ICAM1	IL2RG	paracrine	0.852	FOLR2$^+$ macrophage	Tolerant CD8$^+$ T
TGM2	ITGA4	paracrine	0.818	FOLR2$^+$ macrophage	Tolerant CD8$^+$ T
VCAN	ITGA4	paracrine	0.793	FOLR2$^+$ macrophage	Tolerant CD8$^+$ T
THBS1	ITGA4	paracrine	0.760	FOLR2$^+$ macrophage	Tolerant CD8$^+$ T
VCAN	SELL	paracrine	0.743	FOLR2$^+$ macrophage	Tolerant CD8$^+$ T
CALM2	SELL	paracrine	0.714	FOLR2$^+$ macrophage	Tolerant CD8$^+$ T
CLEC2B	KLRF1	paracrine	0.709	FOLR2$^+$ macrophage	Tolerant CD8$^+$ T

Table S5. Clinical Characteristics of 1405 CRC Patients Involved in This Study. Related to Figure 5.

Characteristics	Number of patients (n =1405)
Cohort	
GSE14333	290 (20.6%)
GSE17536	177 (12.6%)
GSE17537	55 (3.9%)
GSE33113	96 (6.9%)
GSE37892	130 (9.3%)
GSE39582	585 (41.6%)
GSE56699	72 (5.1%)
Gender	
Male	719 (51.2%)
Female	608 (43.3%)
NA	78 (5.5%)
Median age (years)	66.67 (22-97)
Location	
Left	233 (16.6%)
Right	82 (5.8%)
NA	1090 (77.6%)
Satge	
I	66 (4.7%)
II	512 (36.4%)
III	343 (24.4%)
IV	116 (8.3%)
NA	368 (26.2%)
Grade	
I	17 (1.2%)
II	153 (10.9%)
III	34 (2.4%)
NA	1201 (85.5%)
T stage	
Tis	3
T0	1
T1	12 (0.8)
T2	49 (3.5%)
T3	379 (27%)
T4	119 (8.5%)
NA	842 (60%)
N stage	
N0	314 (22.3%)
N1	137 (9.8%)
N2	100 (7.1%)
N3	6 (0.4%)
NA	848 (60.4%)
M stage	
M0	499 (35.5%)
M1	61 (4.3%)
NA	845 (60.2%)
MMR status	
dMMR	77 (5.5%)
pMMR	459 (32.7%)
NA	869 (61.8%)
TP53 status	
Mutation	190 (13.5%)
Wild	161 (11.5%)
NA	1054 (75%)

KRAS status	
Mutation	217 (15.5%)
Wild	328 (23.3%)
NA	860 (61.2%)
BRAF status	
Mutation	51 (3.6%)
Wild	461 (32.8%)
NA	893 (63.6%)
Treatment	
Naive	497 (35.4%)
Chemotherapy	358 (25.5%)
NA	550 (39.1%)

Table S6. Clinical Characteristics of 26 CRC Patients Involved in This Study Related to Figure 1

Characteristics	**Number of patients (n = 26)**
Gender	
Male	11 (42.3%)
Female	15 (57.7%)
Median age (years)	69 (40-89)
Maximum tumor size	
Small (<38 cm²)	19 (73.1%)
Medium (38-69 cm²)	4 (15.4%)
Large (>69 cm²)	4 (15.4%)
Stage	
I	1 (3.81%)
II	13 (50%)
III	11 (42.3%)
IV	1 (3.8%)
Grade	
Low	3 (11.5%)
Low or Moderate	4 (15.4%)
Moderate	15 (57.7%)
High	4 (15.4%)

Data are median (IQR) or n (%).

Table S7. Clinical Characteristics of 181 CRC Patients Involved in This Study. Related to Figure 6.

Characteristics	Number of patients (n = 181)
Gender	
Male	95 (52.5%)
Female	86 (47.5%)
Median age (years)	62 (21-82)
Location	
L-CRC	116 (64.1%)
R-CRC	65 (35.9%)
KRAS Mutation	
Wild	119 (65.7%)
Mutation	62 (34.3%)
Response	
Responder (CR+PR)	118 (65.2%)
Non-responder (SD+PD)	63 (34.8%)

Data are median (IQR) or n (%).
R-CRC = right-sided colorectal cancer; L-CRC, left-sided colorectal cancer.
CR = complete response; PR = partial response; PD = progressive disease; SD = stable disease.

Table S8. Clinical Characteristics of 45 CRC Patients Involved in This Study. Related to Figure 6.

Characteristics	Number of patients (n = 45)
Gender	
Male	27 (60%)
Female	18 (40%)
Median age (years)	66 (25-78)
Location	
LCRC	33 (73.3%)
RCRC	12 (26.7%)
KRAS Mutation	
Wild	28 (62.2%)
Mutation	17 (37.8%)
Response	
Responder (CR+PR)	34 (75.6%)
Non-responder (SD+PD)	11 (24.4%)

Data are median (IQR) or n (%).
R-CRC = right-sided colorectal cancer; L-CRC, left-sided colorectal cancer.
CR = complete response; PR = partial response; PD = progressive disease; SD = stable disease.